

Variation of soil density and earth pressure due to strip compaction

Variation de la densité et de la poussée du sol due à un compactage en bande

Y.S. Fang

Department of Civil Engineering, National Chiao Tung University, Hsinchu, Taiwan

Y.L. Chien

Power Projects, Civil Dept., E & C Corporation, Taipei, Taiwan

ABSTRACT

This paper studies the variation of soil density and earth pressure in a soil mass due to the vibratory compaction along a strip on the surface of the cohesionless backfill. Experiments were conducted in a non-yielding model retaining wall facility and dry Ottawa sand was used as fill material. Based on the test results, it is found that surface settlement increased with the increasing number of passage of the compactor. The relationship between the surface settlement and the number of passes could be properly described by the hyperbolic model. The contours of $\Delta\sigma_v$ after the first passage of the compactor were analogous to a series of concentric circles. As the number of passes increased to 8, the depth of the compaction-induced zone increased with increasing energy input. After the first passage of the compactor, the contours of $\Delta\sigma_h$ formed two regions of stress concentration below the surface. As the number of passage increased to 8, the two high-stress regions merged. The mechanism of soils after the first passage of the compactor could be properly explained by local-shear bearing capacity failure mode. The mechanism of soils after 8 passes of the compactor could be simulated by a single pile driven into a cohesionless soil.

RÉSUMÉ

Cet article étudie les variations de la densité et de la poussée du sol après le compactage par vibration d'une bande à la surface d'un remblai meuble. Des expériences furent réalisées pour étudier les effets d'un vibro-compacteur sur la densification du sol. Basé sur les résultats des essais, la relation entre le tassement de la surface et le nombre de passages du vibro-compacteur pouvait être représentée de manière appropriée par un modèle hyperbolique. Après le compactage, les contours de l'incrément de contrainte verticale $\Delta\sigma_v$ étaient semblables à des cercles concentriques après le premier passage du vibro-compacteur et après 8 passages, et le $\Delta\sigma_v$ diminuait graduellement à partir de la zone centrale de compactage. Les contours de l'incrément de contrainte horizontale $\Delta\sigma_h$ formaient deux zones circulaires de contraintes élevées et $\Delta\sigma_h$ diminuait graduellement à partir de la zone centrale après le premier compactage. Les contours de $\Delta\sigma_h$ étaient semblables à des cercles concentriques après 8 passages du vibro-compacteur. La profondeur de la zone de compaction induite augmentait avec l'accroissement de l'énergie de compactage. Basé sur les résultats des essais, la mécanique des sols du remblai après le premier passage du vibro-compacteur pouvait être simulée à l'aide d'un test de résistance au cisaillement d'une semelle peu profonde. Cependant, après 8 passages du vibro-compacteur, l'interaction entre le compacteur et le sol pouvait alors être simulée par la pénétration d'un pieu carré dans un sol meuble.

Keywords : sand, model test, compaction, settlement, relative density, earth pressure

1 INTRODUCTION

In the construction of highway embankments and earth dams, engineers would compact the loose fill to increase its unit weights. The objective of the compaction operation is to improve the engineering properties of soil such as to increase the bearing capacity or to reduce settlement. Compaction is a particular kind of soil stabilization method and it is one of the oldest methods for improving existing soil or man-placed fills.

To analyze the residual lateral earth pressure induced by soil compaction, several methods of analysis have been proposed by Ingold (1979), Duncan and Seed (1986), Peck and Mesri (1987) and other researchers. However, little information regarding the mechanism of the compacted soil has been reported.

This study simulates the two-dimensional line-compaction with a vibratory compactor on the surface of a loose granular soil in the field. Tests results obtained included the surface settlement, the change of soil density, and the change of stresses in the soil mass due to compaction. Based on the test data, the mechanism of the compacted soil due to the strip compaction on the surface of a sandy soil mass is explored.

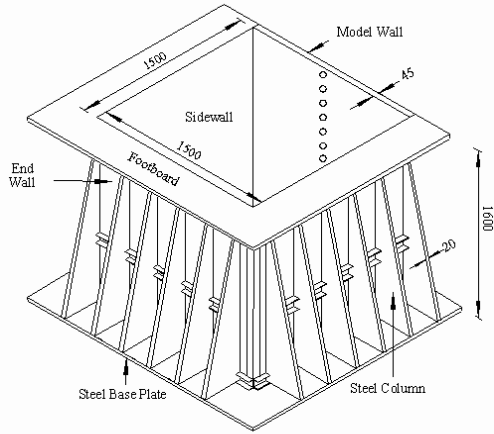
2 EXPERIMENTAL APPARATUS

To investigate the effects of vibratory compaction on a cohesionless soil mass, the instrumented non-yielding model retaining wall facility (Chen and Fang, 2002) at National Chiao Tung University (NCTU) was used.

To constitute a plane strain condition for model testing, the soil bin was designed to minimize the lateral deflection of sidewalls and the friction between the backfill and sidewalls. The soil bin was fabricated of steel plates with inside dimensions of 1500 mm x 1500 mm x 1600 mm as shown in Figure 1. To minimize the friction between the backfill and sidewalls, a lubrication layer consisted of plastic sheets was furnished for all model wall experiments. The lubrication layer proposed by Fang et al. (2004) consisted of one thick and two thin plastic sheets hung vertically on each sidewall of the soil bin before the backfill was deposited.

To investigate the distribution of stresses in the backfill, a series of soil pressure transducers (Kyowa BE-2KCM17, capacity = 98.1 kN/m²) were used. The transducers were buried in the soil mass to measure the variation of vertical and horizontal earth pressure during the filling and compaction process.

To simulate the compaction of loose soil in the field, a vibratory compactor was made by attaching an eccentric motor (Mikasa Sangyo, KJ75-2P) to a 0.225 m × 0.225 m steel plate. The total mass of the vibratory compactor was 12.1 kg. The amplitude of downward cyclic vertical force (static + dynamic) measured with a load cell placed under the base plate of the vibratory compactor was 1.767 kN. The measured frequency of vibration was 44 Hz. Assuming the distribution of contact pressure between the base plate and soil was uniform, the downward cyclic normal stress σ_{cyc} applied to the surface of the soil was 34.9 kN/m².



Unit : mm

Figure 1. NCTU non-yielding model retaining wall and soil bin.

Air-dry Ottawa sand was used as fill material. To simulate the effects of compaction on the surface of a loose fill, the vibratory compactor was pulled over the compaction lane from the left sidewall to the right sidewall as shown in Figure 2. Then the compactor was turned around 180 degrees to compact the same lane for the second pass. At the end, the fill below the compaction lane had been compacted for eight passes with the compactor. The compaction lane was 0.225 m-wide, 1.5 m-long and each pass took 70 seconds.

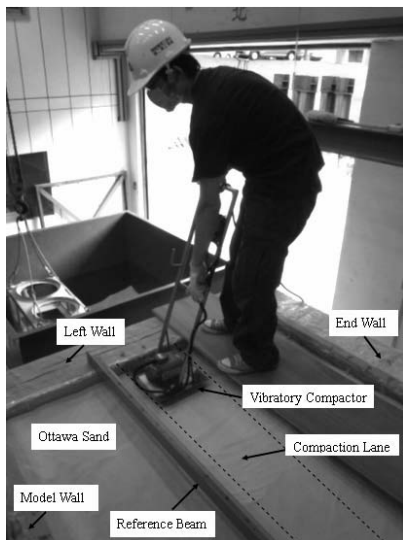


Figure 2. Compaction lane on surface of Ottawa sand.

3 TEST RESULTS

This section reports the variation of the surface settlement, relative density, vertical stress and the horizontal stress due to the strip compaction on the surface of the fill.

Figure 3 shows the surface settlement increased with the increasing number of passes N of the compactor. The surface settlement S shown in Figure 4 was the average settlement of the seven points (point B to H) shown in Figure 3. In Figure 4, the data points obtained from tests 0701 and 0703 indicated that the test results were quite reproducible. Based on the test results, a hyperbolic model was proposed to estimate the surface settlement S as a function of the number of passes of the compactor. The hyperbolic relationship can be expressed as:

$$S = \frac{N}{0.0178 + 0.0241N} \quad (1)$$

where S is the surface settlement in mm, and N is number of passes of the compactor.

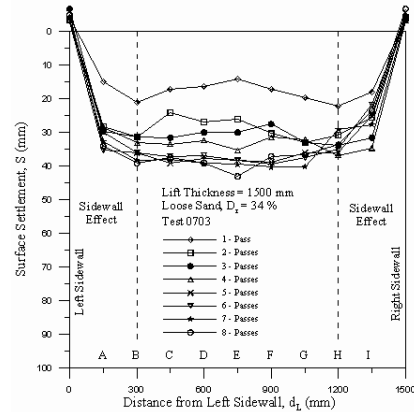


Figure 3. Surface settlement profile of compaction lane.

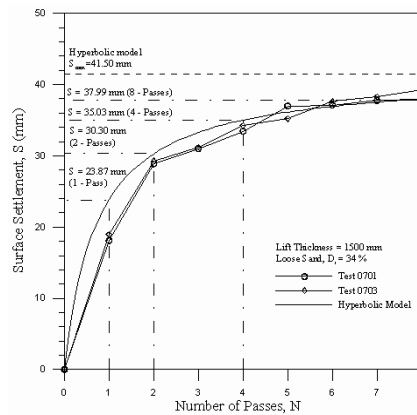


Figure 4. Hyperbolic model to estimate surface settlements S as a function of number of passes of compactor N .

Figure 5 shows the contours of relative density in soil mass after the first passage of the compactor. Before compaction, the fill has a uniform relative density of 34%. Under the compaction lane, the soil density became quite dense ($D_r = 64\%$), and the soil density decreased gradually with the distance from the compaction lane. From the relative density of 34% to 64%, the effects of vibratory compaction on soil density were quite obvious right below the compactor. As the number of passes increased to 8, more compaction energy was transmitted to the soil. In Figure 6, the region of dense sand ($D_r = 72\%$) expanded with the increasing number of the compactor passes. The maximum relative density below the compactor was 75%. The relative density 64% and 75% is corresponding to the dry unit weight 16.3 kN/m³ and 16.6 kN/m³, respectively.

In Figure 7, the contours of $\Delta\sigma_v$ after the first passage of the compactor were analogous to a series of concentric circles. The

center of the concentric circles corresponding to the maximum $\Delta\sigma_v$ was located at the depth of 300 mm below the surface. The $\Delta\sigma_v$ would decrease gradually from the central high-stress region.

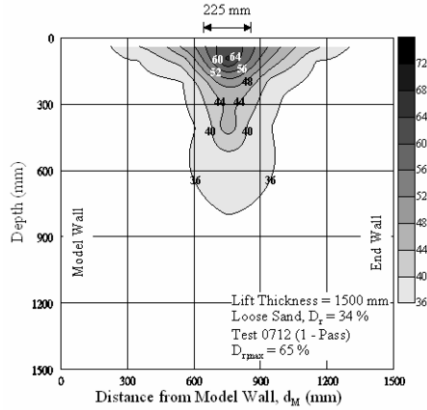


Figure 5. Contours of relative density after 1 – pass of compactor.

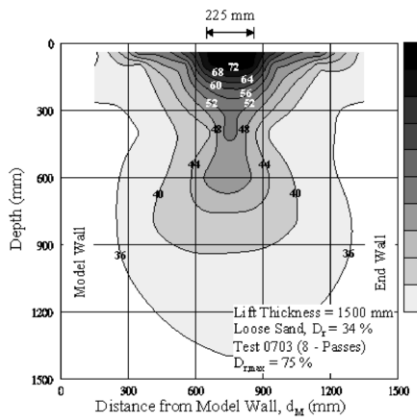


Figure 6. Contours of relative density after 8 – passes of compactor.

Before compaction, vertical stress at the depth of 300 mm calculated by $\sigma_v = \gamma z$ was 4.68 kN/m². The incremental vertical stress $\Delta\sigma_v$ was 2.2 kN/m² and the incremental stress ratio was 53.0%.

In Figure 6, the relative density of soil changed from the initial value 34% to the maximum value of 72%. At $z = 300$ mm, the vertical stress increment due to the change of γ (from 15.6 kN/m³ to 16.6 kN/m³) was 0.30 kN/m². The Comparison between 2.2 kN/m² and 0.30 kN/m², indicated that the vertical stress increment $\Delta\sigma_v$ was not only affected by the change of soil unit weight. The change of vertical stress was related to the compaction-induced stresses.

It may be concluded that the compaction-induced vertical stresses were quite significant below the compaction lane. As the number of passes increased to 8, more compaction energy was input into the soil mass. In Figure 8, the contours showed that the depth of the compaction-induced zone increased with increasing energy input. The vertical stress increment $\Delta\sigma_v$ increased with increasing number of passage of the compactor.

In Figure 9, the contours of $\Delta\sigma_h$ formed two regions of stress concentration at the depth of 300 mm below the surface. Below the peak-stress points, $\Delta\sigma_h$ gradually decreased with increasing depth. At $z = 300$ mm, the initial horizontal stress calculated by Jaky's equation was 2.27 kN/m². The incremental horizontal stress $\Delta\sigma_h$ was up to 1.40 kN/m² and the stress incremental ratio was 62 %. It may be concluded that the compaction-induced horizontal stresses were quite obvious below the compaction lane.

However, as the number of passes of the compactor increased to 8, the double high-stress regions merged, and the contours of $\Delta\sigma_h$ were analogous to a series of concentric circles as shown in Figure 10. It is clear in figures 9 and 10 that the depth of the

compaction-influenced zone increased with increasing compaction energy input.

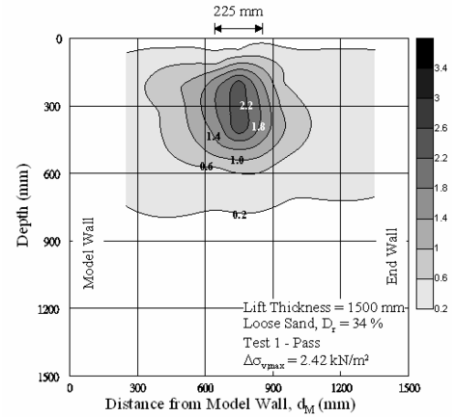


Figure 7. Contours of $\Delta\sigma_v$ after 1 – pass of compactor.

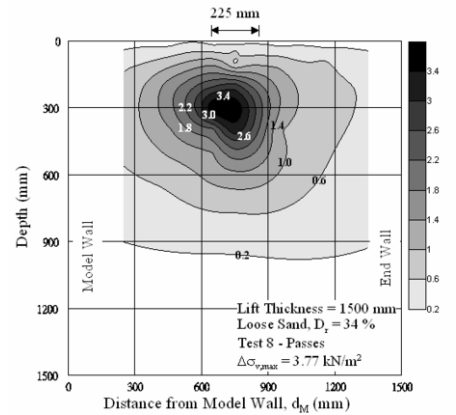


Figure 8. Contours of $\Delta\sigma_v$ after 8 – passes of compactor.

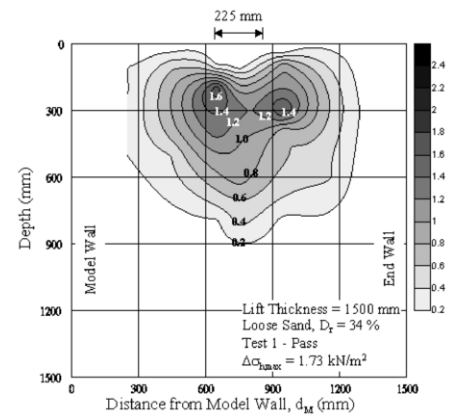


Figure 9. Contours of $\Delta\sigma_h$ after 1 – pass of compactor.

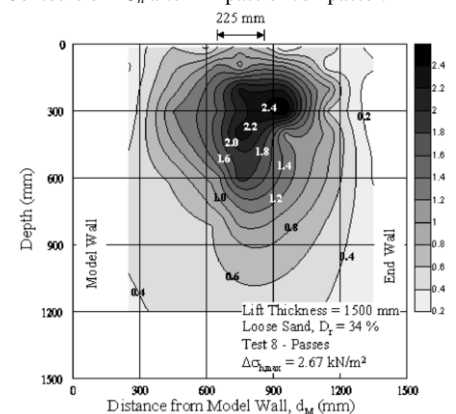


Figure 10. Contours of $\Delta\sigma_h$ after 8 – passes of compactor.

4 MECHANISM OF SOILS UNDER STRIP COMPACTION

Based on the test results reported in previous sections, the mechanism of soils under strip compaction is discussed in this section.

Based on the contours of $\Delta\sigma_h$ in the soil mass after the first passage of the compactor shown in Figure 9, Figure 11 shows the comparison between contours of $\Delta\sigma_h$ in this study and soils under the bearing capacity failure mode (Vesic, 1973). The horizontal stresses under the compactor did not increase which was analogous to the elastic zone under the footing. In Vesic's model, soils in the radial shear zones were pushed by the downward penetration of the footing. In Figure 11, the two high stress zones were thus induced. The mechanism of soils after the first pass of the compactor could be properly explained by local-shear bearing capacity failure mode.

Based on the study of Yang (2006) shown in Figure 12, the influenced range below the pile tip in clean sand would be $3.5D \sim 5.5D$, where D is pile diameter. Calculating the influenced zone of compaction by substituting the compactor width $B = 225$ mm for D , the influence range would be 788 mm \sim 1238 mm. In figure 8 and figure 10, the depth of influence zone for $\Delta\sigma_v$ and $\Delta\sigma_h$ was 800 mm \sim 1200 mm, respectively.

Figure 12 shows both the contours of $\Delta\sigma_h$ measured after 8 passes of the compactor and the influenced zone for a single pile driven in cohesionless soil (Yang, 2006). The influenced zone of compaction is analogous to the stresses below the tip of the pile in cohesionless soil. The mechanism of soils after 8 passes of the compactor could be simulated by a single pile driven in a cohesionless soil.

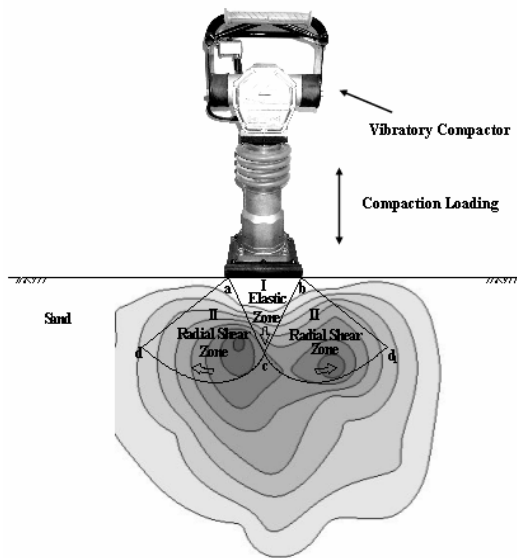


Figure 11. Comparison between horizontal stress increase and local shear failure. (redrawn after Vesic, 1973)

5 CONCLUSIONS

In this study, the effects of strip compaction on sand are investigated. Based on the test results, the following conclusions can be drawn.

1. The surface settlement increased with the increasing number of passes of the compactor. The relationship between the surface settlement and the number of passes of the compactor could be properly described by the hyperbolic model.
2. The contours of $\Delta\sigma_v$ after the first passage of the compactor were analogous to a series of concentric circles. As the number

of passes increased to 8, more compaction energy was input to the soil mass and the depth of the compaction-induced zone increased with increasing energy input.

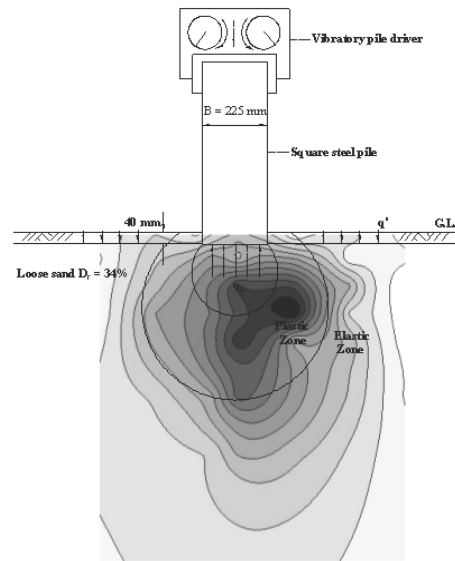


Figure 12. Comparison between test results and influenced zone for a pile driven into sand. (redrawn after Yang, 2006)

3. After the first pass of the compactor, the contours of $\Delta\sigma_h$ formed two regions of stress concentration at the depth of 300 mm below the surface. As the number of passage of the compactor increased to 8, the two high-stress regions merged.
4. The mechanism of soils after the first passage of the compactor could be properly explained by local-shear bearing capacity failure mode. The mechanism of soils after 8 passes of the compactor could be simulated by a single pile driven into a cohesionless soil.

ACKNOWLEDGEMENTS

The writers wish to acknowledge the National Science Council of the Republic China government Grant No. (NSC 95-2221-E-009-199) for the financial assistance that made this investigation possible.

REFERENCES

Chen, T. J., & Fang, Y. S. 2002. A new facility for measurement of earth pressure at-rest. *Geotechnical Engineering Journal*, 3(12): 153-159.

Duncan, J. M., & Seed, R. B. 1986. Compaction-induced earth pressures under K_0 -conditions. *Journal of Geotechnical Engineering*, 112(1): 1-22.

Fang, Y. S., Chen, T. J., Holtz, R. D., & Lee, W. F. 2004. Reduction of boundary friction in model tests. *Geotechnical Testing Journal*, 27(1): 1-10.

Ingold, T. S. 1979. The effects of compaction on retaining walls. *Geotechnique*, 19(3): 265-283.

Peck, R. B. & Mesri, G. 1987. Discussion of Compaction-induced earth pressures under K_0 -conditions. *Journal of Geotechnical Engineering*, 113(11): 1406-1408.

Vesic, A. S. 1973. Analysis of ultimate loads of shallow foundations. *Journal of the Soil Mechanics and Foundations Division*, 99(SM1): 45-73.

Yang, J. 2006. Influence zone for end bearing of piles in sand. *Journal of Geotechnical & Geoenvironmental Engineering*, 132(9): 1229-1237.